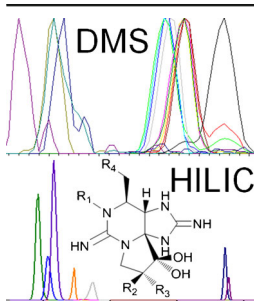


RESEARCH ARTICLE

Differential Mobility Spectrometry for Improved Selectivity in Hydrophilic Interaction Liquid Chromatography-Tandem Mass Spectrometry Analysis of Paralytic Shellfish Toxins

Daniel G. Beach

Measurement Science and Standards, National Research Council Canada, Halifax, NS B3H 3Z1, Canada



Abstract. Paralytic shellfish toxins (PSTs) are neurotoxins produced by dinoflagellates and cyanobacteria that cause paralytic shellfish poisoning in humans. PST quantitation by LC-MS is challenging because of their high polarity, lability as gas-phase ions, and large number of potentially interfering analogues. Differential mobility spectrometry (DMS) has the potential to improve the performance of LC-MS methods for PSTs in terms of selectivity and limits of detection. This work describes a comprehensive investigation of the separation of 16 regulated PSTs by DMS and the development of highly selective LC-DMS-MS methods for PST quantitation. The effects of all DMS parameters on the separation of PSTs from one another were first investigated in detail. The labile nature of 11 α -gonyautoxin epimers gave unique

insight into fragmentation of labile analytes before, during, and after the DMS analyzer. Two sets of DMS parameters were identified that either optimized the resolution of PSTs from one another or transmitted them at a limited number of compensation voltage (CV) values corresponding to structural subclasses. These were used to develop multidimensional LC-DMS-MS/MS methods using existing HILIC-MS/MS parameters. In both cases, improved selectivity was observed when using DMS, and the quantitative capabilities of a rapid UPLC-DMS-MS/MS method were evaluated. Limits of detection of the developed method were similar to those without DMS, and differences were highly analyte-dependant. Analysis of shellfish matrix reference materials showed good agreement with established methods. The developed methods will be useful in cases where specific matrix interferences are encountered in the LC-MS/MS analysis of PSTs in complex biological samples.

Keywords: Ion mobility, Algal toxins, PSP, FAIMS, Selexion, Reference materials

Received: 20 January 2017/Revised: 1 March 2017/Accepted: 2 March 2017/Published Online: 3 April 2017

Introduction

Saxitoxin and its analogues, the paralytic shellfish toxins (PSTs, Figure 1) are potent neurotoxins produced by several species of marine dinoflagellates and freshwater cyanobacteria that are associated with paralytic shellfish poisoning (PSP) [1, 2]. Quantitative analysis of PSTs in shellfish and biological samples is important in safeguarding public health and multi-billion dollar shellfish industries worldwide [3]. Analysis of PSTs is most often carried out with ion-pair reverse phase LC (RPLC) with pre- or post-column oxidation and fluorescence detection [4, 5]. More recently, LC-tandem

mass spectrometry (LC-MS/MS) methods using electrospray ionization (ESI) have been developed [6–10]. Compared with the lipophilic classes of toxins that are routinely quantitated by LC-MS/MS [11, 12], the analysis of PSTs remains a significant instrumental challenge because of their polarity, the large number of structurally similar analogues, including several epimeric pairs (Figure 1), as well as chemical interferences and matrix effects in ESI. Hydrophilic interaction liquid chromatography (HILIC) has emerged as the LC mode of choice and is able to separate all PST analogues with potential to interfere with one another in MS/MS [6–10]. Equally important as selectivity between interfering PST analogues is selectivity between PSTs and interfering matrix components that co-elute in complex biological samples.

Differential mobility spectrometry (DMS) or high-field asymmetric waveform ion mobility spectrometry (FAIMS) was first developed by the Soviet military in the 1980s as a technique for explosives detection, and then later applied to air

Electronic supplementary material The online version of this article (doi:10.1007/s13361-017-1651-x) contains supplementary material, which is available to authorized users.

Correspondence to: Daniel Beach; e-mail: daniel.beach@nrc-cnrc.gc.ca

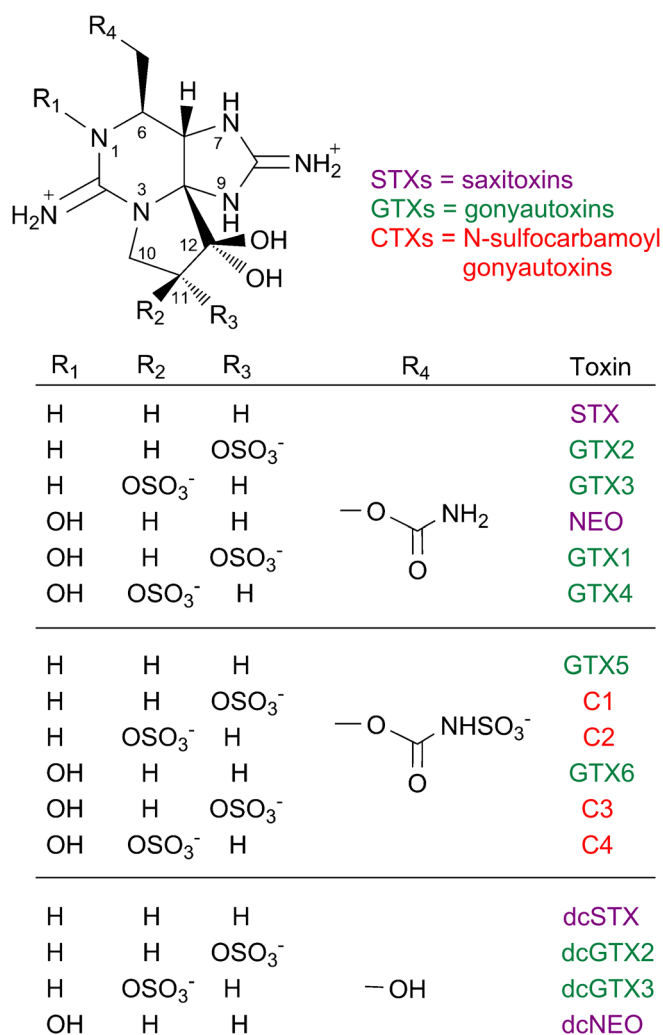


Figure 1. Chemical structures of paralytic shellfish toxins analyzed as part of this study

quality testing in mine safety applications in the West [13, 14]. The technology was fully developed as a separation tool for analytical mass spectrometry at the National Research Council Canada in the late 1990s, and ultimately commercialized [15, 16]. This original FAIMS device commercialized for use with ESI-MS consisted of concentric cylindrical electrodes, and a similar device using planar electrodes was subsequently commercialized by another vendor and dubbed DMS. Though sometimes used interchangeably, here the term FAIMS will be used to refer to analyzers with a cylindrical geometry, and DMS to analyzers with planar geometry. Regardless of geometry, DMS and FAIMS serve as ion filters, separating ions produced by an ion source, at atmospheric pressure, prior to mass spectrometry detection. During this separation, ions travel through the space between two electrodes towards the inlet of a mass spectrometer, through a flow of neutral carrier gas. By applying a high field asymmetric waveform between the two electrodes, the amplitude of which is referred to as dispersion voltage (DV), oscillations of ions are induced in the plane perpendicular to the flow of ions. Differences in ion mobility between species result in different net mobilities over the course of several oscillations, which affect the trajectory

of each species as it passes through the analyzer. This trajectory is based on differential ion mobility, which is related to the shape, size, mass, charge, and polarizability of an ion and is overcome by applying a small DC offset called compensation voltage (CV), which is used analytically to select ions of interest for MS detection. One of the practical advantages of DMS over other formats of linear ion mobility is the degree to which it is possible to tune the selectivity of the separation using a wide range of combinations of voltage and gas conditions. In particular, the use of low % concentrations of polar solvent vapors as chemical modifiers in the carrier gas flow has a dramatic effect on DMS separations and has been used to separate a wide range of chemically and biologically relevant analytes [9, 17–19]. Cylindrical FAIMS devices have the added benefit of ion focusing, which can result in improved selectivity and transmission through the analyzer [20, 21].

Both FAIMS and traveling wave ion mobility spectroscopy (TWIMS) have been investigated for separation of PSTs, with limited success [9, 22, 23]. An original investigation of the separation of PSTs by FAIMS showed good resolution of PSTs from one another using a new prototype FAIMS device, but identified limitations in the commercial device [9]. These included fragmentation of labile PSTs and a slow CV switching time (100 ms) that limited the utility of the LC-FAIMS-MS/MS method developed. TWIMS could separate some STXs (Figure 1) but was only able to achieve partial separation of GTX epimer pairs [22, 23]. ESI-FAIMS-MS has also been previously applied to the analysis of a class of freshwater algal toxin, microcystins, as a direct analysis method without the use of LC [24]. The utility of DMS in combination with LC for the analysis of another polar neurotoxin, β -methylaminoalanine (BMAA) and its isomers has recently been demonstrated, including significant improvements in selectivity and limits of detection over conventional LC-MS approaches [18].

Here, a comprehensive investigation of the behavior of 16 regulated PST analogues was carried out using a planar DMS system. A particular emphasis is placed on exploring conditions leading to fragmentation or transmission of labile PSTs. Conditions optimized for selectivity and sensitivity are then combined with two existing HILIC-MS/MS methods to yield highly selective HILIC-DMS-MS/MS methods. These methods are applied to shellfish reference materials (RMs) containing known quantities of PSTs in order to evaluate qualitative and quantitative performance compared with established methods. This work will be of interest to those analyzing PSTs and serves as an example of the comprehensive optimization required in the development of complex, multi-analyte LC-DMS-MS/MS methods, particularly when both labile and stable analytes need to be monitored simultaneously.

Experimental

Chemicals and Reagents

HPLC grade acetonitrile, methanol, acetone, and 2-propanol were obtained from Caledon (Georgetown, ON, Canada).

Formic acid (for MS, ~98%) and ammonium formate (for MS, >99%) were obtained from Sigma Aldrich (Oakville, ON, Canada). Distilled water was deionized using a Milli-Q system (Millipore, Billerica, MA, USA). Calibration solutions for PSTs were provided by the National Research Council Canada (Measurement Science and Standards, Halifax, NS, Canada) and included the certified reference materials CRM-STX-f, CRM-NEO-c, CRM-GTX1&4-c, CRM-GTX2&3-c, CRM-dcSTX-b, CRM-dcNEO-c, CRM-dcGTX2&3-b, CRM-C1&2-b, and CRM-GTX5-c, as well as in-house reference materials (RMs) for GTX6, C3, and C4.

Samples and Sample Preparation

Shellfish RMs obtained from NRCC included CRM-Zero-Mus, a wet control mussel homogenate certified free from PSTs, and PST positive mussel tissue matrix RMs prepared from mussels blended with toxic algae that have been extensively characterized using LC-PCOX-FLD and LC-MS/MS and found to be homogeneous and stable [25]. A pacific oyster tissue RM was obtained from CEFAS in the UK [26].

Samples were prepared using a dispersive extraction procedure using acetonitrile protein precipitation, as described previously [9]. Tissue homogenate (4.0 g) was vortex mixed with 4.0 mL of 0.1 M HCl and then placed in a boiling water bath for 5 min, cooled, and centrifuged at $6700 \times g$ for 10 min. Final volumes were determined gravimetrically as the sum of extraction solvent and tissue (e.g., 4.0 g + 4.0 mL = 8 mL final volume). A 500 μ L subsample of supernatant was vortex mixed with 500 μ L of acetonitrile to precipitate protein and filtered to 0.45 μ m before analysis.

LC-DMS-MS/MS System

All experimental work was carried out on an Agilent (Mississauga, Ontario, Canada) 1290 LC system coupled to an AB Sciex (Concord, Ontario, Canada) QTRAP 5500 mass spectrometer with a TurboSpray ion source and a Selexion DMS device. The DMS carrier gas modifier delivery system was bypassed, as reported previously [17, 18], and the modifier solvent was delivered using a Harvard (Saint-Laurent, Quebec, Canada) PHD Ultra syringe pump for DMS-MS/MS infusion work or an Agilent 1200 isocratic pump for LC-DMS-MS/MS work. Infusion of PST standards for DMS optimization was carried out using a 10 μ L/min flow of standards (~5 μ M) infused into a 190 μ L/min flow of 1:1 acetonitrile:water with 1 mM ammonium formate and 25 mM formic acid.

Two separate chromatographic methods were used, each with a different set of SRM and DMS parameters. *Method 1* was a rapid UPLC method reported previously for routine analysis of PSTs [8], using a 1.7 μ m BEH amide 2.1 \times 150 mm column (Waters, Milford, MA, USA) held at 60 $^{\circ}$ C and a mobile phase of A = 500:0.075:0.3 water:formic acid:ammonium hydroxide and B = 700:300:0.1 acetonitrile:water:formic acid. The elution gradient parameters are shown in Table 1 and the startup and shutdown column equilibration gradients were operated as reported previously [8]. *Method 2* used a 2 \times 250 mm, 5 μ m amide 80

Table 1. HILIC Gradient Parameters for the Two Chromatographic Methods Used

<i>Method 1: BEH amide</i>			<i>Method 2: amide 80</i>		
Time (min)	Flow rate (μ L/min)	%B	Time (min)	Flow rate (μ L/min)	%B
0	400	95	0	200	90
4	400	95	25	200	55
7.5	400	50	27	200	30
9	500	50	35	200	30
9.3	500	95	50	200	90
9.8	800	95	-	-	-
10.6	800	95	-	-	-
11	400	95	-	-	-

TSK-gel (TosoHaas, Grove City, OH, USA) column held at 40 $^{\circ}$ C, with a mobile phase consisting of A = aqueous 50 mM formic acid with 2 mM ammonium formate and B = acetonitrile, with the elution gradient as shown in Table 1, as reported previously [10]. Mass spectrometry detection was carried out in positive ion selected reaction monitoring (SRM) scan mode using the conditions in Table 2 for DMS optimization studies. Curtain gas was varied in initial DMS optimization work and later optimized at 20 psi for HILIC-DMS-MS/MS experiments. For quantitative HILIC-DMS-MS/MS analysis, scheduled SRM was used to maximize sensitivity for each transition including a 90 s retention time window and a 1 s target cycle time. SRM conditions in Table 2 were used with analysis *Method 1* chromatographic conditions in Table 1. Subsequent work using *Method 2* chromatographic conditions (Table 1) used an alternate approach of varying SRM/DMS parameters in defined retention time windows with a fixed DV of 3500 V, as shown in Table 3.

Results and Discussion

The optimization of the DMS separation of PSTs was undertaken with the goal of improving the selectivity of existing

Table 2. Optimized Method Parameters for HILIC *Method 1*, 0.4% Acetonitrile Carrier Gas Modifier and DV = 3250 V and Scheduled MRM MS/MS Scan Mode

Analyte	R.T. (min)	CV (V)	DP (V)	Precursor <i>m/z</i>	Product <i>m/z</i>	CE (V)
C1	2.6	-7.6	20	493	316	35
C2	2.9	-11.2	20	493	298	40
GTX2	3.7	-15.6	20	396	316	25
GTX1	3.9	-13.6	20	412	332	25
dcGTX2	4.0	-16.4	20	353	273	20
GTX3	4.3	-11.7	120	396	298	25
GTX4	4.5	-13.0	120	412	314	25
dcGTX3	4.6	-13.4	120	353	255	25
GTX5	5.3	-44.0	100	380	300	20
				380	282	25
dcSTX	6.7	-20.0	160	257	239	25
				257	180	35
NEO	6.8	-19.2	160	316	298	25
				316	177	35
STX	6.8	-19.8	140	300	204	35
				300	258	30

Table 3. Optimized Method Parameters for HILIC-DMS-MS/MS *Method 2*, Using Amide 80 Column, 2% Acetonitrile Carrier Gas Modifier, and DV = 3500 V

Period	Compensation voltage (V)	Analyte	Precursor <i>m/z</i>	Product <i>m/z</i>	Collision energy (V)	Dwell time (ms)	
0–23 min	–7.3	C1	493	316	35	200	
			493	298	40	200	
	–11.0	C2	493	298	40	200	
23–26 min	–13.0	GTX1	493	316	35	200	
			412	332	25	100	
	GTX2	412	314	25	100		
		396	316	25	100		
	–11.5	dcGTX2	396	298	25	100	
			353	273	20	100	
		dcGTX3	353	255	25	100	
			396	298	25	100	
		GTX3	396	316	25	100	
			412	314	25	100	
26–28 min	–11.0	GTX4	412	314	25	100	
			412	332	25	100	
	GTX5	380	300	20	200		
		380	282	25	200		
	–7.0	GTX6	396	316	20	200	
			396	298	30	200	
		STX	300	204	35	100	
			300	282	25	100	
	28–35 min	–23.2	dcNEO	273	255	25	100
				273	198	45	100
NEO			316	298	25	100	
			316	177	35	100	
–24.5		dcSTX	257	239	25	100	
			257	180	35	100	

HILIC-MS/MS methods. These methods are already effective at separating PSP isomers from one another, so the primary goal of adding DMS was to separate PSTs from interfering matrix species and chemical background. However, it is not practical to optimize such separations directly since shellfish extract matrix cannot be infused into ESI for DMS optimization because of their complexity and high overall ionic strength, leading to extreme analyte suppression. The more feasible approach is to examine the DMS behavior of a mixture of PST standards under a variety of conditions, taking changes in overall peak capacity of the separation and resolution of PSTs from one another as a proxy measurement of the separation of PSTs from unknown interferents. Once suitable parameters have been established that balance selectivity and sensitivity in DMS-MS, these settings are introduced into existing HILIC methods and the impact of DMS on selectivity can be established.

Despite their common guanidinium backbone, PSTs exhibit a wide range of properties as protonated ions in the gas phase that impact their behavior during DMS and collision induced dissociations (CID). In general, STXs (STX, NEO, dcSTX, dcNEO) are more stable than GTXs (GTX1–6, dcGTX1–4), which are in turn more stable than CTXs (C1–4), as shown in Figure 1. For PSTs with a hydroxysulphate group at the C-11 position, physicochemical properties in the gas phase are additionally dictated by the epimeric position of this group, where 11- α epimers (GTX1, GTX2, dcGTX1, dcGTX2, C1, C3) are highly labile, readily losing sulfur trioxide (SO₃) to form the

[M + H – SO₃]⁺ product ion in positive ionization mode. The more stable 11- β epimers (GTX3, GTX4, dcGTX3, dcGTX4, C2, C4) fragment at much higher energies and preferentially form [M + H – H₂SO₄]⁺ product ions. This behavior has been attributed to interactions between the hydroxysulphate group and the charged guanidinium group in the 11- α epimers that are absent in the 11- β analogues [27].

DMS Optimization

An in-depth investigation of the parameters affecting PST separation by DMS was carried out in order to identify conditions exhibiting the best balance of sensitivity and selectivity for LC-DMS-MS method development. Parameters investigated included DV, type and concentration of carrier gas modifier, throttle gas (enhanced resolution setting), and electrospray polarity. Individual and mixed PST standards were infused into a flow of LC mobile phase, and MS parameters shown in Table 2 were used. For each set of parameters, CV was scanned continuously at scan rates between 0.1 V/s and 0.5 V/s.

Minimal separation was observed among PSTs when pure nitrogen was used as carrier gas and all analogues were transmitted through DMS at CV values between 0 V and 10 V, regardless of the other settings used. These observations indicate that PSTs show similar ion mobility at high and low electric fields and similar differential mobility to one another under “hard sphere” type conditions [14, 19]. Similarly, minimal DMS separation among PSTs was observed in negative ion mode, regardless of carrier gas modifier or other conditions. In order to allow optimization of carrier gas modifier in positive ion mode, a modification was made to the Selexion DMS to allow for external metering of modifier solvent using an LC pump, as reported previously [17, 18]. This modification allows for a full range of modifier concentrations to be added to the carrier gas (0.05% to >5%) and for more uniform evaporation and mixing of the solvent with the gas. A survey of the general impact of different polar solvents acetonitrile, methanol, isopropanol, acetone, water, and ethyl acetate carrier gas modifiers was first carried out using generic DMS conditions. With the exception of water, all solvents showed a significant shift of PST transmission to negative CVs, indicating that effective clustering of ions with neutral solvent molecules was occurring during the low-field portion of the DMS waveform [19]. These preliminary results indicated that acetonitrile showed the best sensitivity and selectivity as a carrier gas modifier for PSTs, and it was therefore investigated in most detail. Isopropanol showed good resolution and sensitivity but also showed multiple peaks for individual PSTs, which made optimization challenging. Acetone showed CV shifts to higher negative values than acetonitrile, but at a greater cost to sensitivity and with no improvement in selectivity between epimers. Methanol showed weaker clustering than acetonitrile and overall poor sensitivity.

Figure 2 shows the impact of introducing various concentrations of acetonitrile vapor into the carrier gas flow on separation of PSP congeners from one another as well as on their

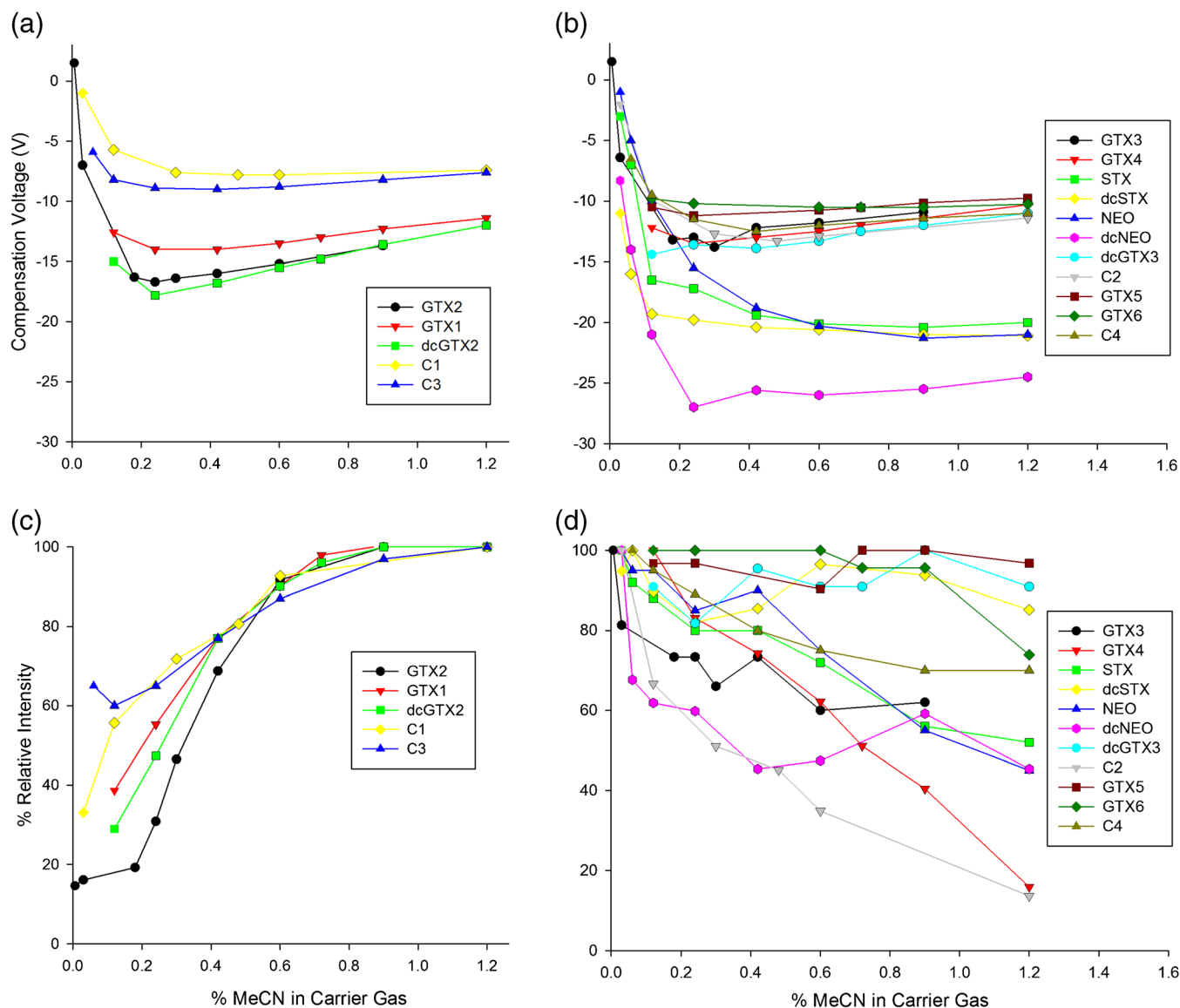


Figure 2. Optimization of acetonitrile modifier concentration in DMS carrier gas with respect to selectivity **(a)**, **(b)** and relative intensity of $[M + H]^+$ precursor in SRM **(c)**, **(d)** of DMS analysis of labile **(a)**, **(c)** and stable **(b)**, **(d)** protonated PSTs at a DV of 3250 V. Intensities in panes c and d are normalized to the most sensitive condition for each analyte

relative sensitivity of detection. In general, increasing the concentration of acetonitrile from 0% leads to a significant negative deviation from $CV = 0$ V up to an analyte-dependant minimum between 0.2% and 0.9% (Figure 2a and b). This is due to increased clustering between analyte ions and neutral solvent molecules during the low-field portions of the waveform, which dissociate under the more energetic conditions of the high-field portion of the waveform. Beyond these concentrations, resolution decreases and some CVs of transmission decrease to less negative values. This can be attributed to reduced declustering during the high field portion of the waveform at higher concentrations of modifier. More complex and analyte-specific trends were observed in changes of relative intensity of $[M + H]^+$ ions with varying the % acetonitrile modifier in the carrier gas (Figure 2c and d). For labile 11- α GTX and CTX epimers, relative intensity increases rapidly

with % modifier up to about 0.8%. This can be attributed to the protective effect of the clustered modifier to field-induced fragmentation in the DMS [28–31], similar to that reported previously for the use of CO_2 as a gas additive in FAIMS [32, 33]. For more stable 11- β epimers (Figure 2d), a decrease in relative intensity with increasing modifier was observed. Decreases in sensitivity with increased modifier have previously been described as resulting from proton transfer reactions between charged analyte and neutral solvent molecules [34]. No significant change in relative intensity was observed for either of the N-sulfocarbamoyl GTXs (GTX 5 or GTX6) or dcGTX3 in Figure 2d, which could either be attributed to the absence or a combination of the above effects.

To investigate the impact of the magnitude of the dispersion field on PST separation, the DV was varied from 2500 V to the instrument maximum of 4100 V with a carrier gas modifier of

0.4% acetonitrile (Figure 3). Below 2500 V, little separation of PSTs was observed. In general, resolution of PST epimers from one another, and overall peak capacity for separation of all PSTs, increased as DV increased, with only small changes in selectivity at low and high DV values (Figure 3a and b). A general trend was observed of CTXs being transmitted at smaller CVs than GTXs that in turn were transmitted at smaller values than STXs, but in most cases some overlap existed between these classes. In general, a decrease in relative sensitivity in DMS is observed with increasing DV and can be attributed to the increased amplitude of oscillations in the DMS resulting in a greater proportion of analyte ions striking the electrodes and being eliminated [30, 31]. For labile PSTs, an even more dramatic decrease in $[M + H]^+$ sensitivity was observed that can be attributed to dissociation within DMS. The degree to which this drop in sensitivity was observed followed similar trends of PST lability as those observed during investigation of modifier concentration. The most labile 11- α CTXs and GTXs gave sharp decreases in $[M + H]^+$ sensitivity and were

practically eliminated at high values of DV (Figure 3c). On the other hand, the more stable STXs showed only a modest decrease in sensitivity at even the highest values of DV (Figure 3d). These more dramatic drops in sensitivity for labile PSTs attributed to dissociation during DMS are investigated in more detail below. Operating the DMS at low DV to maintain sensitivity might initially seem like an attractive option, but the benefits of added selectivity and increasing S/N depend heavily on the increased resolution observed at higher DV values (>2500 V).

The comprehensive investigation of DV at moderate acetonitrile concentration (0.4%) in Figure 3 indicated that improved separation of PSTs can be obtained at higher DV values, but at the cost of sensitivity of labile epimers. The comprehensive investigation of acetonitrile concentration at moderate DV (3250 V) in Figure 2 indicated that increased carrier gas modifier content provided a protective effect for labile epimers, but at the cost of overall selectivity. An additional investigation of the separation of PSTs at high DV (4000 V) and higher acetonitrile concentration (2%) was also carried out and is shown in

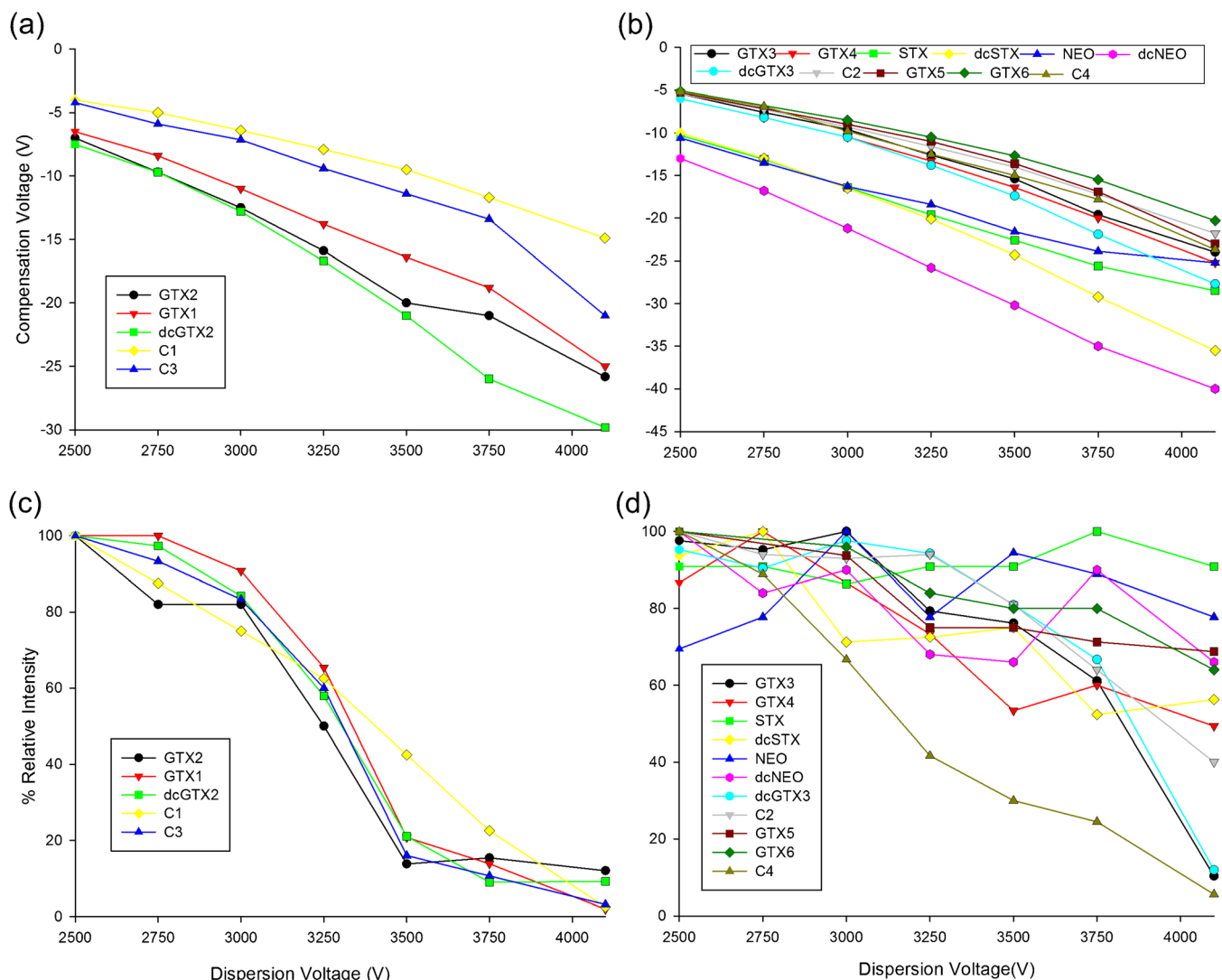


Figure 3. Optimization of DV with respect to selectivity (a), (b) and sensitivity (c), (d) of DMS analysis of labile (a), (c) and stable (b), (d) protonated PSTs using 0.4% acetonitrile as carrier gas modifier

Supplementary Figure S2. At 2% acetonitrile, an increase in DV had comparatively little impact on sensitivity and the same general impact of increased DMS peak capacity (Supplementary Figure S2A). Unlike at lower acetonitrile concentrations, CVs of transmission for PSTs were nearly the same within each class (STXs, GTXs, and CTXs in Figure 1). This has the potential advantage of allowing improved duty cycle in LC-DMS-MS mode, but could also be considered less orthogonal to HILIC, which also separated PSTs into these classes based on charge state in solution. Increasing modifier concentration at DV = 4000 V (Supplementary Figure S2B) in general showed a minor decrease in DMS peak capacity without any major changes in selectivity.

Based on this comprehensive investigation of the separation of PSTs by DMS using acetonitrile as a carrier gas modifier, two sets of parameters were selected as most appropriate for HILIC-DMS-MS/MS method development. CV spectra of a mixture of PST standards at each of these sets of conditions are shown in Figure 4. At moderate DV and acetonitrile concentrations (Figure 4a), the best overall balance of selectivity and sensitivity was obtained at 0.4% acetonitrile and DV = 3250 V. At high DV and acetonitrile concentration (Figure 4b), separation of PSTs into three distinct classes based on their retention time while maintaining acceptable sensitivity was possible at 2% acetonitrile and DV = 3500 V.

The DMS separation of a subset of PSTs from one another has previously been reported using a prototype FAIMS

analyzer [9]. FAIMS and DMS share the same mechanism of separation and the same operating principals, differing only in the geometry of their electrodes (concentric cylinders for FAIMS or flat plates for DMS), and the possibility for ion focusing in FAIMS [20, 21]. Using FAIMS, GTX2 and GTX3 were the most difficult epimer pair to separate, with the maximum resolution of $R = 0.7$ being achieved, while GTX1 and GTX4 were easily baseline separated. Using DMS, GTX2 and GTX3 were baseline separated over a wide range of conditions, but GTX1 and GTX4 were only baseline separated from one another using the “enhanced resolution” setting (Supplementary Figure S2). This setting resulted in decreases in sensitivity of up to 50-fold (Supplementary Figure S2), as reported previously for other analysis of plant hormones by DMS [35], limiting its utility for most applications. This setting introduces a countercurrent throttle gas that slows the flow of ions towards the mass spectrometer and increases the residence time of ions in the analyzer and the number of DV cycles ions experience. The observed drop in sensitivity can be attributed to decreased ion transmission due to a combination of diffusive loss, charge transfer from analytes to neutrals, and analyte neutralization on electrodes.

The differences observed between the separation of PSTs by DMS here and FAIMS previously [9] can be attributed to differences in electrode geometry, residence time, dispersion field, analyzer temperature, and carrier gas composition. These characteristics and parameters have an impact on selectivity, resolution, and ion transmission.

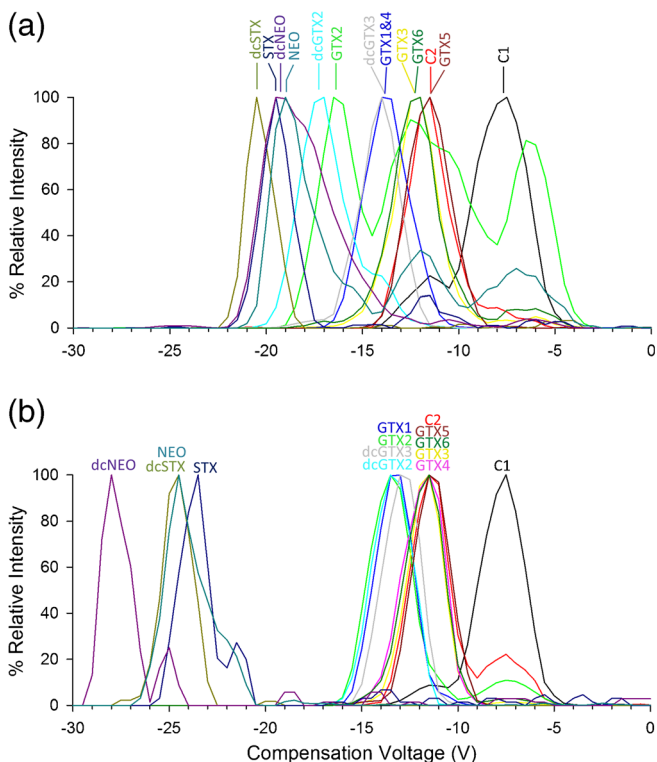


Figure 4. DMS separation of a mixed PST standard using a carrier gas modifier of 0.4% acetonitrile and DV = 3250 V (a) and 2% acetonitrile and DV = 3500 V (b). SRM parameters are as described in Table 1

Fragmentation of Labile PSTs Before, During and After DMS

Controlling the dissociation of PSTs before, during, and after DMS is central to their successful analysis by this technique and it was desirable to investigate these effects in more detail. In all cases, monitoring the SO_3 elimination fragment $[M + H - 80]^+$ of sulphated PST epimers showed an increase in this fragment as DV increased or as % acetonitrile decreased. A detailed example of this effect is shown in Figure 5 for a mixture of GTX2 and GTX3 epimers. The % acetonitrile modifier was increased from 0 to 1% (Figure 5a) at a moderate DV of 3250 V. Full separation of the epimers is observed at 0.2% acetonitrile, but the more labile GTX2 is detected predominantly as its $[M + H - \text{SO}_3]^+$ dissociation product. At 0.5% acetonitrile, the protective effect of the acetonitrile shows similar intensities of the precursor and product ions, and the additional clustering of the added modifier leads to their partial resolution. At 1% acetonitrile, GTX2 is predominantly present as its protonated precursor and the fragment is completely separated by DMS. The intensity and CV of transmission of the more stable GTX3 changes relatively little compared with GTX2, though the best overall resolution between GTX2 and GTX3 is observed near 0.4% acetonitrile (Figure 2). By contrast, an increase in DV from 2900 V to 3700 V at a moderate acetonitrile concentration (Figure 5b) showed a sharp decrease

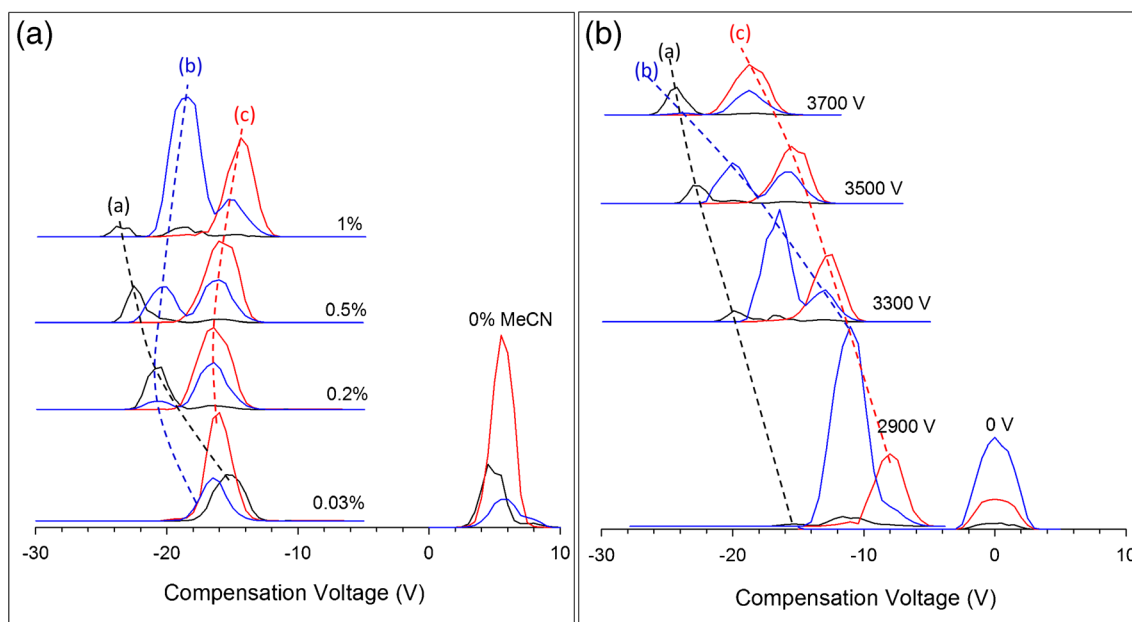


Figure 5. Fragmentation and separation of GTX2, GTX3 (m/z 396) and their SO₃ loss dissociation product (m/z 316) at varying concentrations of acetonitrile carrier gas modifier at a DV of 3250 V **(a)** and varying DV at 0.6% acetonitrile modifier **(b)**. Analyte peak labels correspond to GTX2 **(b)**, GTX3 **(c)**, and the DMS induced SO₃ loss fragment primarily originating from GTX2 **(a)**

in the intensity of the GTX2 precursor ion and a corresponding increase in the $[M + H - SO_3]^+$ dissociation product transmitted at a larger negative CV value. This, along with the fact that

comparatively little intensity of the GTX3 precursor is lost demonstrates that labile PSTs are susceptible to DV-induced dissociation during DMS.

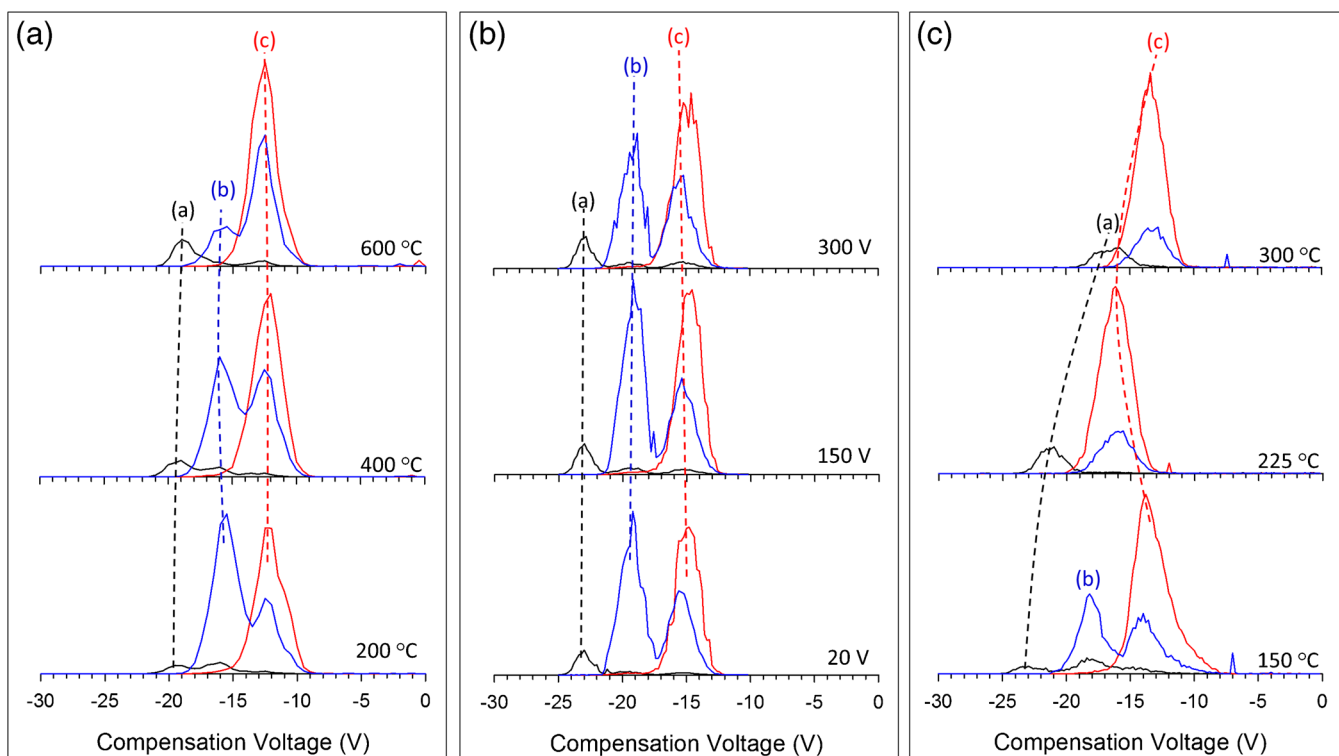


Figure 6. DMS separation of GTX2 and GTX3 while varying DMS-MS parameters affecting fragmentation of labile PSTs including turbospray temperature (T_{ESI}) **(a)**, DV **(b)**, and DMS temperature (T_{DMS}) **(c)**. Pane a used 0.4% acetonitrile modifier, $T_{DMS} = 150$ °C, and DP values from Table 1. Pane b used 0.6% acetonitrile modifier, $T_{ESI} = 275$ °C, and $T_{DMS} = 150$ °C. Pane c used 1% acetonitrile modifier, $T_{ESI} = 275$ °C, and DP values from Table 1. Analyte peak labels correspond to GTX2 **(b)**, GTX3 **(c)**, and the DMS induced SO₃ loss fragment primarily originating from GTX2 **(a)**

Three peaks are observed in the CV spectrum of the SO_3 loss transition of GTX2/3 in Figure 5, each with a distinct origin in the ESI-DMS-MS process. Regardless of the DV or modifier settings used, two of these peaks are always transmitted at the same CV as their precursors, suggesting typical source fragmentation; collision induced dissociation in the inlet to mass spectrometer. At appropriate conditions, such as the 1% trace in Figure 5a, the third $[\text{M} + \text{H} - \text{SO}_3]^+$ peak is transmitted through DMS at a distinct CV from either GTX2 or GTX3, indicating fragmentation before or during the DMS separation. It is important to note that fragmentation before and during DMS are not distinguished by CV of transmission [31]. Assuming precursor and product ions are transmitted at different CVs, once the product ion is exposed to the CV of the precursor, it will strike an electrode and be eliminated. Fragmentation during DMS can, however, have an impact on ion transmission, particularly when there is a large difference in CV between precursor and product ions [31].

In order to further investigate this effect, other MS and DMS parameters expected to impact in-source fragmentation were investigated for analysis of a mixture of GTX2 and GTX3, as shown in Figure 6. Increasing electrospray ionization temperature (Figure 6a) induces thermal dissociation of labile GTX2 before DMS, resulting in an increase in the $[\text{M} + \text{H} - \text{SO}_3]^+$ peak transmitted at $\text{CV} = -19.5$ V. On the other hand, in-source fragmentation induced by an increase in dispersion potential (Figure 6b) does not result in an increase in the $[\text{M} + \text{H} - \text{SO}_3]^+$ peak transmitted at $\text{CV} = -23$ V in Figure 6b. This is because the DP is applied at the inlet to mass spectrometry, after the DMS separation. The relatively small increase in the $[\text{M} + \text{H} - \text{SO}_3]^+$ transmitted at the same CV as the $[\text{M} + \text{H}]^+$ ions of GTX2 and GTX3 in Figure 6b can be attributed to the relative insensitivity of the QTRAP 5500 to DP induced in-source dissociation in general. Finally, fragmentation of GTX2 can also be induced during the DMS separation by increasing the temperature in the analyzer (T_{DMS}), as shown in Figure 6c. It has previously been shown that T_{DMS} and field strength have an additive effect in inducing dissociation in DMS [28, 31]. Unlike altering ESI or MS inlet conditions, increasing T_{DMS} leads to a change in the dynamics of the DMS separation and thus in CV of transmission. Increasing T_{DMS} beyond the minimum setting of 150°C leads to complete loss of GTX2 and deterioration of separation. Unfortunately, settings for T_{DMS} are limited to 150°C , 225°C , and 300°C , making it unlikely that this setting is optimized for the detection of labile analytes, even at its lowest setting.

Another parameter often expected to impact in-source fragmentation is the curtain gas used for desolvation of ESI droplets, which opposes the flow of ions toward the MS orifice. In the case where DMS is used, the curtain gas is drawn into the space between the DMS electrodes and serves as the DMS carrier gas. Unlike the settings examined in Figure 5, increasing the curtain gas did not increase fragmentation of labile PSTs, but using a lower value of 20 psi gave significant improvement in overall sensitivity compared with higher values

(Supplementary Figure S3). This can be attributed to improved dynamics of ion probing and has also been reported for other small polar analytes [18]. Interestingly, the opposite trend was observed for PST analysis on the same instrument without DMS installed, where a higher value of 40 psi was found to be optimum in terms of sensitivity and prevented instrument contamination. Here, the protective effect of the DMS prevented contamination of the MS ion optics even when a low curtain gas setting is used.

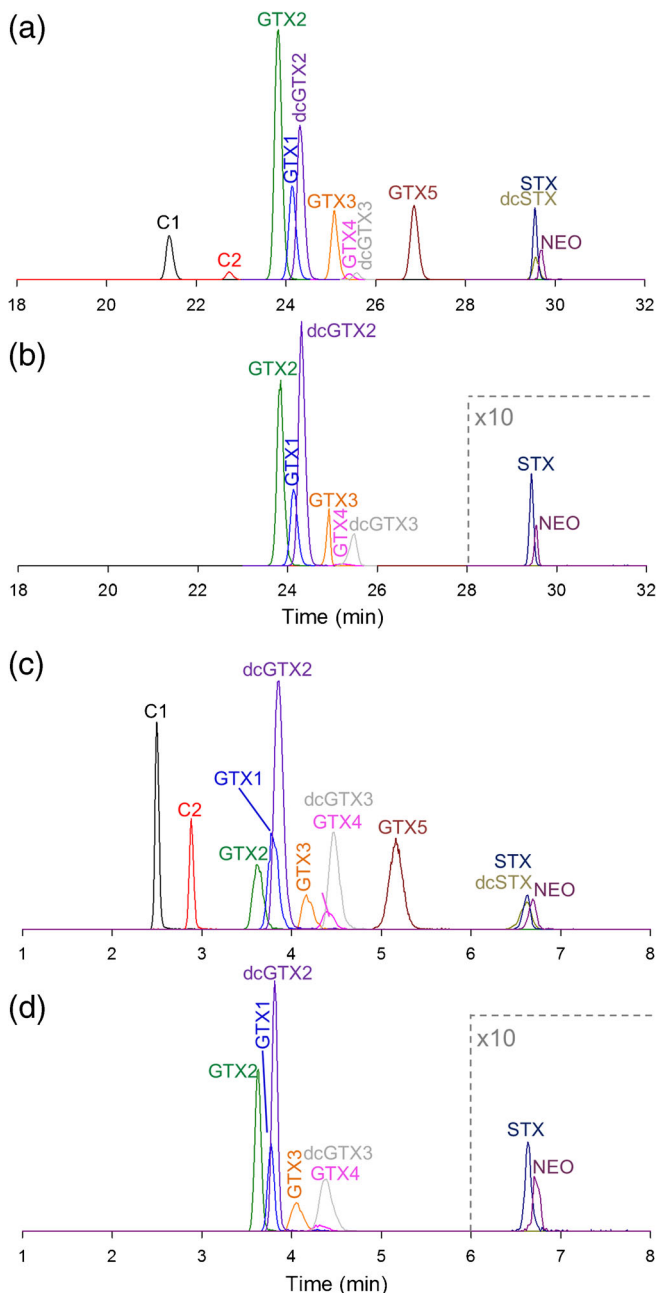


Figure 7. HILIC-DMS-MS/MS analysis of a mixed PSP standard (a), (c) and a mussel tissue reference material (b), (d) using *Method 1* using a $5\ \mu\text{m}$ amide 80 column, retention time scheduling, and SRM conditions in Table 2 (a), (b) and *Method 2* using a $1.8\ \mu\text{m}$ BEH amide column and SRM conditions in Table 3 (c), (d)

LC-DMS-MS/MS Method Development

Two different HILIC methods using different columns, both with amide functionality, have emerged as the most suitable for LC separation of PSTs. *Method 1* uses a 1.8 μm particle size BEH amide column, a rapid 10 min gradient, and has been validated with an activated carbon SPE cleanup for routine food safety testing applications [8, 36]. *Method 2* uses a 5 μm particle size amide 80 column and has been widely used for a range of research purposes since 2005 [6]. This method offers the best resolution of

PSTs with excellent method robustness, but is relatively slow. Here, both HILIC gradients were investigated for use in a HILIC-DMS-MS/MS method with the optimized DMS conditions identified above (Figure 4), both using SRM scan mode.

Once a CV value is assigned to a particular SRM transition, only species sharing CV of transmission, precursor ion m/z , and product ion m/z are detected in that CV/SRM transition. As described previously for BMAA [18], the sensitivity of HILIC-DMS-MS/MS methods are limited by the duty cycle of

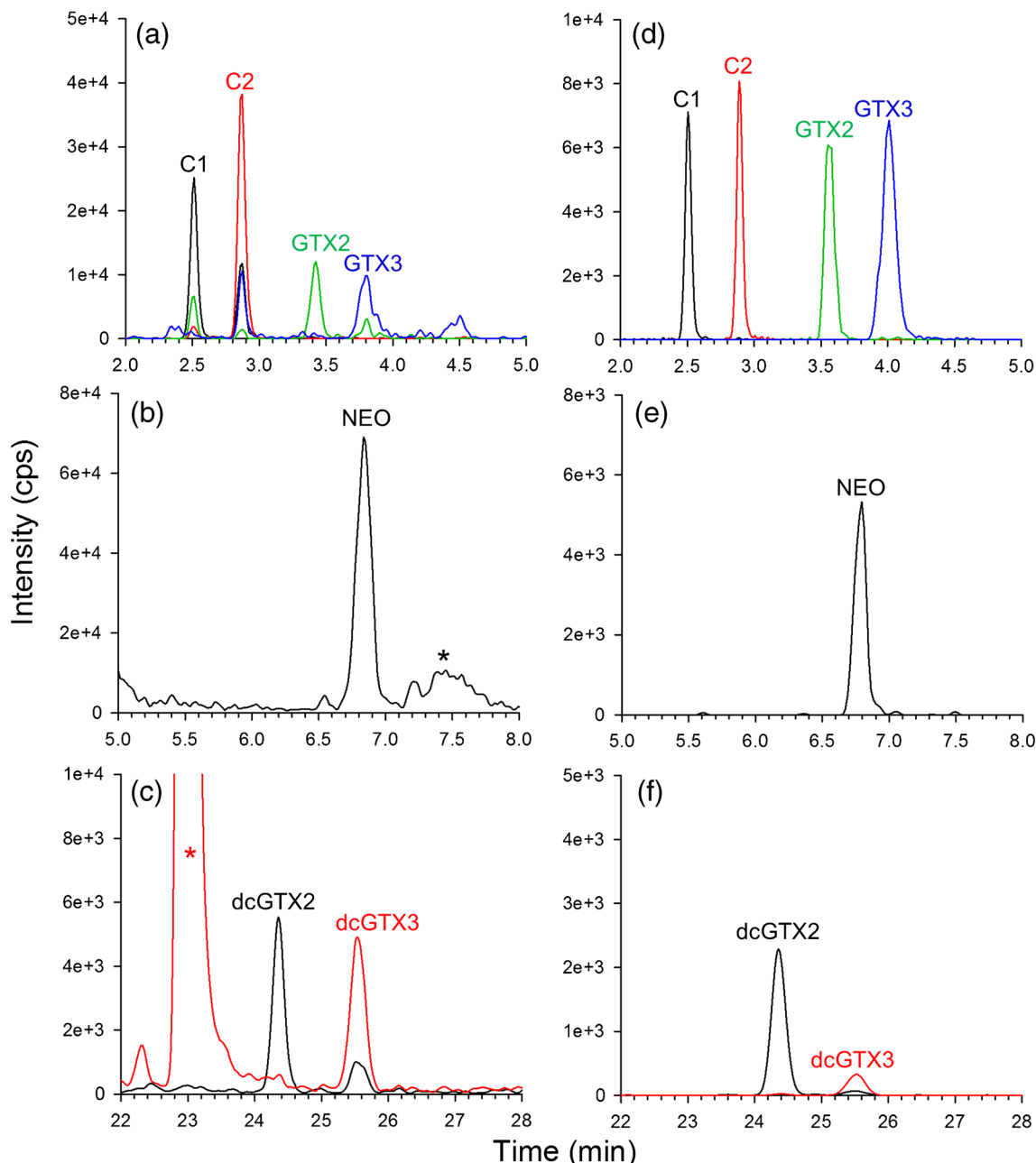


Figure 8. Improvements in selectivity between HILIC-MS/MS (a), (b), (c) and HILIC-DMS-MS/MS (d), (e), (f) for CRM-PO-PST (a), (d) and RM-PSP-Mus Pilot (b), (e) analyzed using *Method 1* using a 5 μm amide 80 column and SRM conditions in Table 2 and a spiked control mussel tissue sample analyzed using *Method 2* using a 1.8 μm BEH amide column and SRM conditions in Table 3 (b), (d). Asterisks denote potentially interfering matrix peaks. Retention time scheduling was not used in order to show background peaks

switching between multiple CV values (minimum 20 ms), and limits of detection are proportional to the number of CV/SRM transitions monitored. This was particularly challenging for comprehensive detection of a large number of PST congeners, each with multiple SRM transitions requiring very fast dwell times in HILIC-MS/MS. Two options were investigated to deal with this limitation. Retention time scheduling was simple to implement, requiring only knowledge of the retention times of targeted PSTs, and was applicable to any DMS conditions selected (Table 2). An alternative approach was also investigated using the high DV/high modifier conditions shown in Figure 4b. Here, CVs of transmission converged on three values, corresponding to the classes shown in Figure 1: STXs, GTXs, and CTXs. Since these classes also elute in non-overlapping retention time windows, it was possible to significantly limit the number of CV/SRM transitions that needed to be monitored in each window (Table 3). This method was somewhat more complicated to set up and data from multiple retention time windows was less convenient to process than scheduled SRM data.

Figure 7 shows HILIC-DMS-MS/MS chromatograms for the analysis of a PST standard mixture using the amide 80 method (Figure 7a) and the BEH amide method (Figure 7c). Both approaches showed similar and improved sensitivity and LOD compared with using HILIC-DMS-MS/MS and SRM without retention time scheduling (not shown).

The developed methods were applied to the analysis of shellfish tissue RM and spiked control samples with well characterized concentrations of PSTs to determine the impact of DMS on selectivity and sensitivity. Figure 7b and d show analysis of a mussel tissue matrix material that contains a subset of the PSTs examined using the two developed methods. The impact of the sample matrix on peak shape and HILIC retention time are evident, but because of the added selectivity of DMS there is a notable absence of matrix background. Examples of improvements in selectivity between methods with and without DMS are shown in Figure 8. Figure 8a demonstrates the general improvement in selectivity that was observed throughout, including an elimination of chemical background originating from the electrospray process and an elimination of matrix peaks. In both HILIC-MS/MS methods, unknown matrix interference peaks occur immediately following elution of the STXs, in particular NEO, which are effectively eliminated by DMS (Figure 8b). For the *Method 2*, another area of potential matrix interference exists in transitions for dcGTX2/3, which is also effectively eliminated by DMS (Figure 8c).

The biggest limitation of DMS in general is the significant decrease in sensitivity (ion counts) observed compared with methods without DMS, which is evident in Figure 8. For DMS to be beneficial, this loss in sensitivity must be offset by an increase in selectivity, resulting in an increase in signal-to-noise. However, in other cases where selectivity of the original method was adequate, little to no benefit is observed when using DMS. It is therefore important to evaluate differences in signal-to-noise and LOD between methods with and without DMS when evaluating the utility of the technique for a

particular application. In general, both methods offered significantly improved selectivity compared with HILIC-MS/MS. *Method 1* using scheduled SRM, 0.4% acetonitrile, and DV = 3250 V was selected for further investigation because of ease of use and maximum selectivity.

Quantitative Capabilities of LC-DMS-MS/MS Method 1

The quantitative performance of *Method 1* was evaluated with respect to a number of common validation parameters, and compared with the performance of an equivalent HILIC-MS/MS method without DMS installed. This evaluation was based on the quantitation of three shellfish tissue RMs using matrix matched calibration. A mussel tissue matrix RM certified free of PSTs was used for matrix matching experiments and to assess selectivity. Good linearity ($R^2 \geq 0.99$) was observed for matrix matched standards over the calibration ranges shown in Table 4. Limits of detection (Table 4) were estimated ($S/N = 3$) based on signal-to-noise ratios observed from analysis of low-level matrix matched standards. The impact of using DMS on LOD was highly analyte-dependant and related to the DMS parameters chosen as well as the chemical background from ESI and matrix peaks observed in each transition. For some analytes (C1, GTX1) a significant improvement in LOD is observed whereas for others (C2, GTX4) better performance is observed by HILIC-MS/MS, but in most cases LODs were comparable using methods with and without DMS.

Concentrations determined in the three shellfish tissue RMs were in good agreement with values assigned using reverse phase LC with fluorescence, and HILIC-MS/MS in the case of PSP-Mus (Supplementary Figure S4). In particular, good agreement was observed between analyses with and without DMS using the current methodology, indicating that any deviation from assigned values are likely due to differences in sample preparation and calibration rather than the instrumental method used. Method precision was evaluated as standard

Table 4. Calibration Range and Limits of Detection for PST Analysis Using HILIC-DMS-MS/MS *Method 1* Compared with Those for an Equivalent HILIC-MS/MS Method Without DMS

Analyte	HILIC-DMS-MS/MS <i>Method 1</i>		HILIC-MS/MS	
	Calibration range (nM)	LOD (nmol/kg)	Calibration range (nM)	LOD (nmol/kg)
C1	5.2–1273	3.2	16–1273	27
C2	1.6–391	7.6	5–391	3
GTX2	1.6–397	25	15–397	40
GTX1	2.2–529	14	20–529	116
dcGTX2	3.6–878	7.4	11–878	26
GTX3	1.6–131	15	15–131	42
GTX4	6.5–175	181	19–175	39
dcGTX3	1.2–287	8	11–287	33
GTX5	4.7–382	27	14–382	19
dcSTX	33–893	240	33–893	476
NEO	13–1032	111	38–1032	364
STX	12–998	144	37–998	663

Retention Time Scheduling was Used for Both Methods

deviations of triplicate analyses, shown in Supplementary Figure S4, and was comparable with typical HILIC-MS/MS analysis of PSTs.

Conclusion

This paper has demonstrated the detailed investigation of DMS parameters required for comprehensive optimization of a multi-analyte HILIC-DMS-MS/MS method. For PSTs, the need to simultaneously detect highly labile and relatively stable analytes further complicates optimization and led to a detailed investigation into instrument parameters that induce analyte dissociation before, during, and after DMS separation. Increasing DV and DMS temperature were the most important parameters leading to analyte fragmentation while increasing the concentration of acetonitrile modifier in the carrier gas had a significant protective effect on labile PSTs.

Optimized DMS parameters were combined with two existing HILIC-MS/MS methods to create highly selective HILIC-DMS-MS/MS methods. These were used to analyze shellfish tissue RMs and shown to be significantly more selective than methods without DMS. Quantitative performance of the developed method was comparable to HILIC-MS/MS for analysis of PSTs in shellfish tissue RMs. Because of the significant cost to sensitivity of using DMS, differences in limits of detection were highly analyte dependant and did not offer a significant overall improvement. The developed HILIC-DMS-MS/MS methods will be useful in cases where specific selectivity problems are identified in the HILIC-MS/MS analysis of PSTs in shellfish. Future improvements by instrument manufacturers in DMS ion transmission and probing will lead to further improvements to the developed methodology.

Acknowledgements

Thanks to Krista Thomas, Elliott Kerrin, and Kelley Reeves for technical assistance as well as Pearse McCarron and Michael Quilliam for editorial input. Thanks also to Gary Glish and Brandon Santiago of UNC Chapel Hill for valuable discussions and their presentation on analyte dissociation in DMS at the Lake Louise Tandem Mass Spectrometry Workshop.

References

1. Wiese, M., D'Agostino, P.M., Mihali, T.K., Moffitt, M.C., Neilan, B.A.: Neurotoxic alkaloids: saxitoxin and its analogs. *Mar. Drugs* **8**, 2185–2211 (2010)
2. Vale, P.: In: Botana, L.M. (ed.) Saxitoxin and analogs: ecobiology, origin, chemistry, and detection. CRC Press, Boca Raton (2014)
3. Isabella Sanseverino, D.C., Pozzoli, L., Dobricic, S., Lettieri, T.: Algal bloom and its economic impact. EUR 27905 EN. Joint Research Centre, Ispra (2016)
4. van de Riet, J.M., Gibbs, R.S., Chou, F.W., Muggah, P.M., Rourke, W.A., Burns, G., Thomas, K., Quilliam, M.A.: Liquid chromatographic post-column oxidation method for analysis of paralytic shellfish toxins in mussels, clams, scallops, and oysters: single-laboratory validation. *J. AOAC Int.* **92**, 1690–1704 (2009)
5. Lawrence, J.F., Niedziadek, B., Menard, C.: Quantitative determination of paralytic shellfish poisoning toxins in shellfish using prechromatographic oxidation and liquid chromatography with fluorescence detection: collaborative study. *J. AOAC Int.* **88**, 1714–1732 (2005)
6. Dell'Aversano, C., Hess, P., Quilliam, M.A.: Hydrophilic interaction liquid chromatography-mass spectrometry for the analysis of paralytic shellfish poisoning (PSP) toxins. *J. Chromatogr. A* **1081**, 190–201 (2005)
7. Blay, P., Hui, J.P.M., Chang, J., Melanson, J.E.: Screening for multiple classes of marine biotoxins by liquid chromatography-high-resolution mass spectrometry. *Anal. Bioanal. Chem.* **400**, 577–585 (2011)
8. Boundy, M.J., Selwood, A.I., Harwood, D.T., McNabb, P.S., Turner, A.D.: Development of a sensitive and selective liquid chromatography-mass spectrometry method for high throughput analysis of paralytic shellfish toxins using graphitised carbon solid phase extraction. *J. Chromatogr. A* **1387**, 1–12 (2015)
9. Beach, D.G., Melanson, J.E., Purves, R.W.: Analysis of paralytic shellfish toxins using high-field asymmetric waveform ion mobility spectrometry with liquid chromatography-mass spectrometry. *Anal. Bioanal. Chem.* **407**, 2473–2484 (2015)
10. Li, A., Ma, J., Cao, J., Wang, Q., Yu, R., Thomas, K., Quilliam, M.A.: Analysis of paralytic shellfish toxins and their metabolites in shellfish from the North Yellow Sea of China. *Food Addit. Contam. Part A* **29**, 1455–1464 (2012)
11. van den Top, H.J., Gerssen, A., McCarron, P., van Egmond, H.P.: Quantitative determination of marine lipophilic toxins in mussels, oysters and cockles using liquid chromatography-mass spectrometry: inter-laboratory validation study. *Food Addit. Contam. Part A* **28**, 1745–1757 (2011)
12. McNabb, P., Selwood, A.I., Holland, P.T., Aasen, J., Aune, T., Eaglesham, G., Hess, P., Igarishi, M., Quilliam, M., Slattery, D., Van de Riet, J., Van Egmond, H., Van den Top, H., Yasumoto, T.: Multiresidue method for determination of algal toxins in shellfish: single-laboratory validation and interlaboratory study. *J. AOAC Int.* **88**, 761–772 (2005)
13. Shvartsburg, A.A.: Differential ion mobility spectrometry. CRC Press, Boca Raton (2008)
14. Schneider, B.B., Nazarov, E.G., Londry, F., Vouros, P., Covey, T.R.: Differential mobility spectrometry/mass spectrometry history, theory, design optimization, simulations, and applications. *Mass Spectrom. Rev.* **35**, 687–737 (2016)
15. Purves, R.W., Guevremont, R.: Electrospray ionization high-field asymmetric waveform ion mobility spectrometry-mass spectrometry. *Anal. Chem.* **71**, 2346–2357 (1999)
16. Guevremont, R.: High-field asymmetric waveform ion mobility spectrometry: a new tool for mass spectrometry. *J. Chromatogr. A* **1058**, 3–19 (2004)
17. Purves, R.W., Ozog, A.R., Ambrose, S.J., Prasad, S., Belford, M., Dunyach, J.-J.: Using gas modifiers to significantly improve sensitivity and selectivity in a cylindrical FAIMS device. *J. Am. Soc. Mass Spectrom.* **25**, 1274–1284 (2014)
18. Beach, D.G., Kerrin, E.S., Quilliam, M.A.: Selective quantitation of the neurotoxin BMAA by use of hydrophilic-interaction liquid chromatography-differential mobility spectrometry-tandem mass spectrometry (HILIC-DMS-MS/MS). *Anal. Bioanal. Chem.* **407**, 8397–8409 (2015)
19. Schneider, B.B., Covey, T.R., Coy, S.L., Krylov, E.V., Nazarov, E.G.: Chemical effects in the separation process of a differential mobility/mass spectrometer system. *Anal. Chem.* **82**, 1867–1880 (2010)
20. Guevremont, R., Purves, R.W.: Atmospheric pressure ion focusing in a high-field asymmetric waveform ion mobility spectrometer. *Rev. Sci. Instrum.* **70**, 1370–1383 (1999)
21. Purves, R.W., Prasad, S., Belford, M., Vandenberg, A., Dunyach, J.-J.: Optimization of a new aerodynamic cylindrical FAIMS device for small molecule analysis. *J. Am. Soc. Mass Spectrom.* Just accepted, doi: 10.1007/s13361-016-1587-6 (2017)
22. Poyer, S., Loutelier-Bourhis, C., Coadou, G., Mondeguer, F., Enche, J., Bossée, A., Hess, P., Afonso, C.: Identification and separation of saxitoxins using hydrophilic interaction liquid chromatography coupled to traveling wave ion mobility-mass spectrometry. *J. Mass Spectrom.* **50**, 175–181 (2015)
23. Poyer, S., Loutelier-Bourhis, C., Toggetti, V., Joubert, L., Enche, J., Bossée, A., Mondeguer, F., Hess, P., Afonso, C.: Differentiation of gonyautoxins by ion mobility-mass spectrometry: a cationization study. *Int. J. Mass Spectrom.* **402**, 20–28 (2016)

24. Ells, B., Froese, K., Hrudey, S.E., Purves, R.W., Guevremont, R., Barnett, D.A.: Detection of microcystins using electrospray ionization high-field asymmetric waveform ion mobility mass spectrometry/mass spectrometry. *Rapid Commun. Mass Spectrom.* **14**, 1538–1542 (2000)
25. Reeves, K., Thomas, K., Quilliam, M.A.: In: Henshilwood, K., Deegan, B., McMahon, T., Cusack, C., Keaveney, S., Silke, J., O’Cinneide, M., Lyons, D., Hess, P. (eds.) A mussel tissue certified reference material for paralytic shellfish poisoning toxins. The Marine Institute, Galway (2006)
26. Turner, A.D.: Certificate of analysis pacific oyster PSP toxin matrix CRM (PO PST CRM 1101). Centre for Environment, Fisheries, and Aquaculture Science: Weymouth, UK (2012) Available at: <http://citeseerx.ist.psu.edu/viewdoc/download?doi=10.1.1.259.6867&rep=rep1&type=pdf> Accessed January 05 (2017)
27. Dörr, F.A., Kovačević, B., Maksić, Z.B., Pinto, E., Volmer, D.A.: Intriguing differences in the gas-phase dissociation behavior of protonated and deprotonated gonyautoxin epimers. *J. Am. Soc. Mass Spectrom.* **22**, 2011–2020 (2011)
28. An, X., Eiceman, G.A., Rodriguez, J.E., Stone, J.A.: Gas phase fragmentation of protonated esters in air at ambient pressure through ion heating by electric field in differential mobility spectrometry. *Int. J. Mass Spectrom.* **303**, 181–190 (2011)
29. Kandler, S., Lambertus, G.R., Dunietz, B.D., Coy, S.L., Nazarov, E.G., Miller, R.A., Sacks, R.D.: Fragmentation pathways and mechanisms of aromatic compounds in atmospheric pressure studied by GC-DMS and DMS-MS. *Int. J. Mass Spectrom.* **263**, 137–147 (2007)
30. Veasey, C.A., Thomas, C.L.: Fast quantitative characterisation of differential mobility responses. *Analyst* **129**, 198–204 (2004)
31. Santiago, B.G., Campbell, M.T., Glish, G.L.: Characterization of variables affecting internal energy deposition inside a differential ion mobility spectrometer. *J. Am. Soc. Mass Spectrom.* Submitted, (2017)
32. Ells, B., Barnett, D.A., Purves, R.W., Guevremont, R.: Detection of nine chlorinated and brominated haloacetic acids at part-per-trillion levels using ESI-FAIMS-MS. *Anal. Chem.* **72**, 4555–4559 (2000)
33. Lyczko, J., Beach, D., Gabryelski, W.: Detection, identification, and occurrence of thiotetronic acids in drinking water from underground sources by electrospray ionization-high field asymmetric waveform ion mobility spectrometry-quadrupole time-of-flight-mass spectrometry. *Anal. Chem.* **87**, 9884–9891 (2015)
34. Blagojevic, V., Koyanagi, G.K., Bohme, D.K.: Multi-component ion modifiers and arcing suppressants to enhance differential mobility spectrometry for separation of peptides and drug molecules. *J. Am. Soc. Mass Spectrom.* **25**, 490–497 (2014)
35. Pang, N., Yan, C.: Study of field mobilities dependence and direct separation of acidic phytohormones by differential mobility spectrometry–mass spectrometry. *Int. J. Mass Spectrom.* **362**, 48–55 (2014)
36. Turner, A.D., McNabb, P.S., Harwood, D.T., Selwood, A.I., Boundy, M.J.: Single-laboratory validation of a multitoxin ultra-performance LC-hydrophilic interaction LC-MS/MS method for quantitation of paralytic shellfish toxins in bivalve shellfish. *J. AOAC Int.* **98**, 609–621 (2015)